Ecological Informatics 5 (2010) 492–502

Contents lists available at ScienceDirect

Ecological Informatics

journal homepage: www.elsevier.com/locate/ecolinf

Uncertainty analysis of eddy flux measurements in typical ecosystems of ChinaFLUX

Honglin He [a], Min Liu [a,b], Xiaomin Sun [a], Li Zhang [a], Yiqi Luo [c], Huiming Wang [a], Shijie Han [d], Xinquan Zhao [e], Peili Shi [a], Yanfen Wang [b], Zhu Ouyang [a], Guirui Yu [a,*]

[a] Key Laboratory of Ecosystem Network Observation and Modeling, Institute of Geographic Sciences and Natural Resources Research, Chinese Academy of Sciences, Beijing 100101, China
[b] Graduate University of Chinese Academy of Sciences, Beijing 100049, China
[c] Department of Botany and Microbiology, University of Oklahoma, 770 Van Vleet Oval, Norman, OK 73019, USA
[d] Institute of Applied Ecology, Chinese Academy of Sciences, Shenyang, Liaoning 110016, China
[e] Northwest Plateau Institute of Biology, Chinese Academy of Sciences, Xining, Qinghai 810001, China

ARTICLE INFO

Article history:
Received 9 January 2010
Received in revised form 6 July 2010
Accepted 9 July 2010

Keywords:
Eddy covariance
Measurement error
Random error
Flux
Uncertainty
ChinaFLUX

ABSTRACT

Fluxes of CO_2 (FCO_2) and energy (latent heat, LE; sensible heat, H) exchange between ecosystems and atmosphere, as measured by the eddy covariance technique, represent a fundamental data source for global-change research. However, little is known about the uncertainties of flux measurements at an ecosystem level in China. Here, we use data from six eddy covariance tower sites in ChinaFLUX, including two forested sites, three grassland sites, and one agricultural site, to conduct a cross-site analysis of random flux errors (RFEs) of FCO_2, LE, and H. By using the daily-differencing approach, paired observations are obtained to characterize the random error in these measurements. Our results show that: (1) The RFEs of FCO_2, LE, and H in different ecosystems of ChinaFLUX closely follow a double-exponential (Laplace) distribution, presumably due to a superposition of Gaussian distribution for high flux magnitude. (2) The RFEs of FCO_2, LE, and H are not homogeneous and appear to be a linear function of flux magnitude. (3) Except for H, the RFEs of FCO_2 and LE exhibit a distinct seasonal pattern. For FCO_2, the dependence of RFEs on wind speed varies somewhat according to vegetation type, whereas for LE and H, there is no such dependence. The effect of temperature on RFEs is not statistically significant ($P<0.05$). Both the distribution and the relationship of RFEs with flux magnitude in ChinaFLUX are essentially in accord with those in AmeriFlux and CarboEurope.

1. Introduction

The long-term and continuous eddy covariance (EC) measurements of ecosystem fluxes such as CO_2, water, and energy between biosphere and atmosphere at tower sites around the world (e.g., Baldocchi et al., 2001; Yu et al., 2006; Mizoguchi et al., 2009) offer various opportunities to improve our understanding about the fundamental processes of ecosystem functions in both time and space (Baldocchi, 2003; Friend et al., 2007). However, there is a growing recognition within the eddy-flux community that more attention needs to be paid to the uncertainties inherent in these EC measurements (Hollinger and Richardson, 2005; Richardson et al., 2006; Lasslop et al., 2008). With the development of a model-data fusion method in terrestrial ecosystem research, data uncertainties are as important as data themselves and play a major role in determining the outcome (Raupach et al., 2005). Therefore, how to quantify the uncertainty of flux data and acquire the probability density function (PDF) and its statistical characteristics have become a frontier issue in global flux research.

Flux data actually are not deterministic; rather, they can be expressed as the "correct" value plus or minus measurement error, which is called uncertainty. Specifically, a flux measurement (x) represents a sum of the "true" flux (F) and the potential measurement errors, which can be further divided into systematic errors (ε) and random measurement errors (δ), namely $x = F + \varepsilon + \delta$ (Richardson et al., 2006). The systematic errors and random measurement errors are usually evaluated separately. The energy imbalance and incomplete nocturnal data may cause the systematic errors, which are difficult to identify. However, the systematic errors can be eliminated by calculating the bias. Identifying the source of systematic error and how to reduce this error represent an active research area in flux study (Goulden et al., 1996; Moncrieff et al., 1996; Mahrt, 1998; Twine et al., 2000; Massman and Lee, 2002; Morgenstern et al., 2004). In contrast to systematic error, random error is related to the observational systems (e.g., gas analyzers, ultrasonic apparatus, data acquisition system, and the calculation method), turbulent transport, and the heterogeneity in flux footprint (Moncrieff et al., 1996). In most cases, random measurement errors cannot be eliminated, but their numerical value can be obtained by statistic analysis. Here, as regards the uncertainty of flux observation data, we mainly focus on RFEs.

Extensive studies on the random errors of EC data have been conducted by a repeated sampling method in a single tower or twin towers (Hollinger and Richardson, 2005; Richardson et al., 2006; Rannik et al., 2006) or statistical analysis of model residuals (Hagen et al., 2006; Chevallier et al., 2006; Lasslop et al., 2008). Hollinger and Richardson

* Corresponding author. Tel.: +86 010 6488 9268; fax: +86 010 6488 9399.
E-mail address: yugr@igsnrr.ac.cn (G. Yu).

1574-9541/$ – see front matter © 2010 Elsevier B.V. All rights reserved.
doi:10.1016/j.ecoinf.2010.07.004

(2005) studied flux data uncertainty by using repeated sampling method in two nearby towers in Howland Forest, pointing out that random measurement error follows a double-exponential (Laplace) distribution rather than a normal (Gaussian) distribution. Meanwhile, a daily-differencing approach was proposed to quantify the RFEs in a single tower (Hollinger and Richardson, 2005). Rannik et al. (2006) discussed the uncertainty of flux observation data through use of the repeated-sampling method at the same time in two nearby towers (within a distance of 30 m) in Hyytiala of Finland. Richardson et al. (2006) conducted a cross-site study on flux measurement errors in AmeriFlux, including forest, grassland, and farmland ecosystems. They demonstrated that flux measurement errors of different ecosystems follow a double-exponential distribution as well. The relationships between measurement errors and environment variables and flux magnitudes are also examined. Based on model residuals, Richardson et al. (2008) conducted a systematic analysis of the statistical characteristics of CO_2 flux random errors in several forest ecosystems in Europe, and they suggested that the random error analysis method based on model residuals is a supplement to the daily-differencing approach based on single (double)-tower data.

Based on these investigations, a number of studies on parameter optimization and model-data fusion were conducted (Richardson and Hollinger, 2005; Hagen et al., 2006; Lasslop et al., 2008). Regarding analysis of random measurement error, Richardson and Hollinger (2005) compared the effects of two different error distributions (Gaussian distribution versus double-exponential distribution) on model parameter selections. They also explored the relationship between random error and environment factors using the maximum likelihood method for parameter optimization. Hagen et al. (2006) conducted uncertainty analysis of gross ecosystem exchange (GEE) derived from 7 y of continuous eddy covariance measurements in Howland Forest. In China, Liu et al. (2009) analyzed the random error of CO_2 flux measurements, and they employed the bootstrapping method to evaluate different models and optimization methods in influencing the estimate of key parameters and CO_2 flux components. Zhang et al. (2008) explored the effect of error distribution of CO_2 flux on key parameters in ecosystem carbon-cycle models. However, the statistical properties of random measurement errors remain currently under debate and need to be tested and verified at more flux towers around the world (Richardson et al., 2006; Lasslop et al., 2008; Williams et al., 2009).

This paper seeks to obtain the statistical characteristics of RFEs for FCO_2, LE, and H; quantify the uncertainty of flux data; determine its influencing factors; and compare the differences of the RFEs among ChinaFLUX, AmeriFlux, and CarboEurope. Data used in our analyses are from six sites in ChinaFLUX, including two forested sites, three grassland sites, and one agricultural site. We first focus on evaluating the statistical characteristics and distribution of RFEs in CO_2 and energy (latent energy, LE and sensible heat, H). Then we examine the relationship between RFEs and flux magnitude as well as wind speed. The seasonality of RFEs and the influence of temperature on the random error in all three fluxes are also discussed. Finally we compare our results with similar studies for the AmeriFlux and CarboEurope. All these works tend to provide technical support for quantifying flux observation uncertainty and properly evaluating flux observations, which in turn will be helpful for model-data fusion research and model evaluation.

2. Data and method

2.1. Data

Data used in our analyses are obtained from six eddy covariance sites within the ChinaFLUX network, representing a diverse range of ecosystems: subtropical evergreen coniferous plantation (QYZ), northern warm temperate deciduous broad-leaved forest (CBS), Qinghai-Tibet Alpine meadow (HBGC), Qinghai-Tibet alpine grassland meadow (DX), Inner Mongolia typical grassland (NM), and Huang-Huai-Hai farmland (YC). The flux and routine meteorological measurements are operated with the same set of instruments and program at the six forest sites (Yu et al., 2006). For most sites, at least 3 or 4 y of continuous measurements are available. An overview of these sites is given in Table 1. Extensive data and site information are available online at the ChinaFLUX Web site (http://www.chinaflux.org/).

The datasets are processed by using the flux data processing system at ChinaFLUX (Li et al., 2008). The processing includes: (1) coordinate rotation for 30-min flux data (Wilczak et al., 2001), (2) Webb–Pearman–Leuning (WPL) correction (Webb et al., 1980; Leuning, 2004), (3) storage calculation for forested sites (Hollinger et al., 1994), (4) outlier rejection (Papale et al., 2006), and (5) nighttime filtering with u^* threshold obtained by evaluating the relationship between temperature and CO_2 flux (Reichstein et al., 2005).

2.2. Method

2.2.1. Determination of flux uncertainty

Uncertainty associated with the measured eddy covariance flux can be defined as the variance of high-frequency data in average time (e.g., 30 min), which can be detected by taking multiple measurements when the data are relatively independent and the condition is stable and then using the variability of these measurements to estimate the standard deviation. However, flux is usually not stable, because of the influence of phenologic and climate conditions. Therefore, simultaneous measurements from two towers located nearby can be used to meet the assumption of the repeated-sampling method (Hollinger and Richardson, 2005; Rannik et al., 2006). Given the fact that there are very few sites where two adjacent towers can simultaneously measure fluxes for the same ecosystem in ChinaFLUX, we use the daily-differencing approach as described by Hollinger and Richardson (2005) to quantify the random measurement errors. Specifically, a measurement pair (x_1, x_2) is considered valid only if both measurements are made under "equivalent" environmental conditions (PPFD within 75 μ mol m^{-2} s^{-1}, air temperature within 3 °C, and wind speed within 1 m/s) in the same successive two days. These criteria are chosen as a trade off for two conflicting requirements: (1) environmental conditions sufficiently similar that the difference between the measured fluxes can be attributed to random error instead of the differences in forcing variables; and (2) a large enough set of measurement pairs to accurately characterize the probability distribution function (PDF) of the random error (Richardson et al., 2006). Regarding the limitation of sampling length, the sample should be obtained for more than 1 y. We use $(x_1\text{-}x_2)/\sqrt{2}$ to express the measurement errors, δ. The standard deviation of random errors is used to characterize flux measurement uncertainty. Finally, we can estimate the RFEs by calculating the standard deviation of the differences, which is expressed as:

$$\sigma(\delta) = \frac{\sigma(x_1 - x_2)}{\sqrt{2}} \tag{1}$$

2.2.2. Analysis of the RFEs

According to the traditional micrometeorologic method based on turbulence theory (Lenschow et al., 1994; Mann and Lenschow, 1994), the relationship between random measurement error and environmental variables can be described as:

$$\sigma \propto |\overline{F}| \sqrt{\frac{h_\tau}{\bar{u}T}} \tag{2}$$

where $|\overline{F}|$ is the absolute value of mean flux, h_τ is the appropriate height measure for the integral timescale, $\bar{u}$ is the mean wind speed at the measurement height, and T is the sampling period (e.g., $T = 1800$ s for our study). From Eq. (2), we can expect that the flux magnitude and wind speed may be the main factors influencing random measurement error.

In this study, we focus on the scaling of RFEs with $|\overline{F}|$ and $\bar{u}$. The inferred random errors are divided into many bins on the basis of flux

Table 1
Site information for forested, grassland, and agricultural site in ChinaFLUX.

Site	Abbreviations	Long. (°E)	Lat. (°N)	Vegetation type	Elevation (m)	Measurement height (m)	Period
Qianyanzhou	QYZ	115.07	26.73	Sub-tropical planted forest	100	23.6	2003–2006
Changbaishan	CBS	128.10	42.40	Temperate deciduous mixed forest	738	41.5	2003–2006
Haibeiguancong	HBGC	101.32	37.60	Alpine shrub	3293	2.2	2003–2006
Dangxiong	DX	91.08	30.85	Alpine meadow	4333	2.2	2004–2006
Neimeng	NM	117.45	43.50	Temperate steppe	1187	2.5	2004–2006
Yucheng	YC	116.60	36.95	Maize field, summer Wheat field, winter	28	2.2	2003–2006

Table 2
Statistical properties of the inferred RFEs in FCO_2, LE and H for CBS site (2003–2006) during different time of the year and different time of the day.

Flux	Time	Number of observations	Mean	Standard deviation	Skewness	Kurtosis
FCO_2 (μmol m^{-2} s^{-1})	Day	1712	−0.03	2.89	0.27	14.91
	Night	651	−0.22	1.91	0.00	8.27
	Growing season (DOY102-295)	1324	−0.15	3.48	0.28	9.59
	Dormant season	1039	0.00	0.80	−0.17	5.63
	All	2363	−0.08	2.66	0.28	15.74
LE (W m^{-2})	Day	2113	0.56	36.10	0.00	13.86
	Night	1594	1.28	27.11	1.34	76.52
	Growing season (DOY102-295)	1783	0.88	44.50	0.23	15.60
	Dormant season	1924	0.87	14.34	1.01	82.14
	All	3707	0.87	32.54	0.33	27.82
H (W m^{-2})	Day	2213	−0.18	26.24	−0.22	7.99
	Night	1623	0.37	18.43	−0.56	9.03
	Growing season (DOY102-295)	1855	−0.25	24.90	−0.50	9.78
	Dormant season	1981	0.33	21.61	−0.02	7.13
	All	3836	0.05	23.26	−0.31	8.97

magnitude with an equal number of data points, and the standard deviation ($\sigma(\delta)$) is calculated accordingly. Furthermore, an analysis of variance (ANOVA) is conducted on the resulting data set by calculating $\sigma(\delta)$ for each vegetation type across all possible bins of environment variables ($\overline{F}\times\bar{u}$), with each $|\overline{F}|$ and $\bar{u}$ as ANOVA factors. When it comes to explaining the seasonality of uncertainty, we group the RFEs into 12 bins according to month. The mean value of flux magnitude, environment variables, and the standard deviation of random error ($\sigma(\delta)$) for each group are calculated. Finally, a partial correlation analysis is conducted to illustrate the inherent relationship between RFEs and environment factors.

3. Results

3.1. Statistical characteristics of RFEs

3.1.1. Statistical properties

After estimating RFEs for six sites by using the daily-differencing approach, statistical properties (e.g., the mean, standard deviation, kurtosis, and skewness) of the inferred random error, $\delta = (x_1 - x_2)/\sqrt{2}$, are calculated. The mean values of δ for each of FCO_2, LE, and H are close to zero (Table 2, exemplary for the CBS site). Whereas the standard deviations of the flux differences $\sigma(\delta)$ among FCO_2, LE, and H also have been shown to vary from site to site (Table 3), especially in relation to vegetation type and environment factors (e.g., time of the year and time of the day). For FCO_2, the $\sigma(\delta)$ ranges from 0.3 to 5.0, for LE from 9.2 to 49.8, and for H from 15.7 to 43.9. The overall $\sigma(\delta)$of LE tends to be somewhat larger than that in H during the growing season. YC appears to be an exception, while the random error in H (40.3 W m^{-2}) is higher than that in LE during the maize season (35.6 W m^{-2}). For both FCO_2 and LE across all sites, RFEs are larger during daytime than at night, and larger during the growing season than the rest of the year, whereas these tendencies are not obvious in H.

RFEs for FCO_2, LE, and H in both carbon and energy fluxes at grassland sites are smaller compared with forested sites. For example, during daytime, RFEs in FCO_2 are roughly 4-fold larger at QYZ ($\sigma(\delta)$=3.91 μmol m^{-2} s^{-1}) than that at HBGC ($\sigma(\delta)$=0.93 μmol m^{-2} s^{-1}), and the RFEs in H at NM are twice as large as that at DX. In cropland ecosystems, as the maize-growing season is more productive, the RFE in FCO_2 ($\sigma(\delta)$=5.0) appears to be about 2.5-fold larger than that during wheat-growing

Table 3
Random flux errors ($\sigma(\delta)$) estimation in FCO_2 , LE, and H at different sites during different time of the year and different time of the day.

Flux	Time	QYZ	CBS	HBGC	NM	DX	YC
FCO_2 (μmol m^{-2} s^{-1})	Day	4.10	2.89	0.94	0.85	0.58	4.19
	Night	1.70	1.91	0.91	0.88	0.53	2.65
	All	3.91	3.48 (G)	1.11 (G)	1.00 (G)	0.69 (G)	5.00 (G)
			0.80 (D)	0.29 (D)	0.45 (D)	0.29 (D)	1.87 (D)
LE (W m^{-2})	Day	49.77	36.10	20.93	36.33	21.54	31.11
	Night	34.97	27.11	21.03	34.35	30.69	22.63
	All	48.14	44.50 (G)	30.30 (G)	36.12 (G)	32.59 (G)	35.64 (G)
			14.34 (D)	9.16 (D)	34.92 (D)	16.06 (D)	21.14 (D)
H (W m^{-2})	Day	31.70	26.24	25.91	38.00	23.29	31.06
	Night	18.27	18.43	19.15	36.15	27.62	39.25
	All	30.31	24.9 (G)	24.34 (G)	28.75 (G)	15.72 (G)	40.3 (G)
			21.61 (D)	24.37 (D)	43.85 (D)	28.39 (D)	25.56 (D)

Note: G: Growing season (DOY102-295 in CBS; DOY115-300 in HBGC; DOY123-280 in NM; DOY123-289 in DX); D: Dormant season; M: Maize season (DOY 161-275) and W: Wheat season in YC.

season ($\sigma(\delta)$=1.9). Furthermore, even among forested sites there tends to be a substantial variation in RFEs, and the RFEs of FCO_2, LE, and H at QYZ clearly are higher than that at CBS, which may be related to localized climate conditions at these two forested sites.

3.1.2. Probability distribution

For all sites, and for each of FCO_2, LE, and H, the error distributions clearly follow a non-normal distribution, with a very tight central peak but also very heavy tails (Fig. 1c, g, k). The skewness of the RFEs is close to zero (Table 2, exemplary for CBS site), suggesting that the RFEs across all sites are close to symmetric distribution. Compared with normal (Gaussian) distribution, the double-exponential (Laplace) distribution tends to provide a better description of the error, especially with an excess kurtosis (for FCO_2, kurtosis >8, for LE, kurtosis >12, and for H, kurtosis >8, Table 4), while for normal distribution the kurtosis is equal to 3, and a high kurtosis indicates a strong peak. However, the distribution of the RFEs varies from site to site, and the error distribution does not perform well for all sites. The Kolmogorov–Smirnov test of normality is used for random measurements errors at all sites. The diagnostic test shows that random measurements errors are not normally distributed (P<0.01). Therefore, compared with the normal distribution, double-exponential distribution can provide a better fit to the random error. The high peak in the double-exponential distribution means that the small error has a higher frequency than the normal distribution, and thick tails depict that the big error also has a higher frequency than the normal distribution.

However, if we group RFEs according to the flux magnitude, we find a normal distribution for high flux magnitude in FCO_2 and H, while for LE the distribution is between Gaussian and Laplace distribution (see Fig. 1a, e, i, exemplary for CBS site). When adding more data, the distribution is rather double-exponential. With regard to the RFEs, we have confirmed with our data that the double-exponential distribution of RFEs is largely due to a superposition of normal distribution, especially for FCO_2 and H. Furthermore, pursuing another possibility to show the normal distribution of RFEs, we normalize the RFEs (error-mean of the error/standard deviation of the error) with the standard deviation derived within a time window of seven days, which transforms all error distributions to a standard deviation of unity. For FCO_2 and H, the normalized errors are closer to normal distribution (Fig. 1, d, l), whereas for LE, the normalized error distribution is more peaked (Fig. 1h). For FCO_2, LE, and H, the normalized errors reduce the kurtosis and largely change the distribution to a less-peaked shape compared with the original distribution (Table 4).

3.2. Relationship between RFEs, flux magnitude, and wind speed

From Eq. (2), it appears that the inferred random flux error can be attributed to the flux magnitude (F) and wind speed ($\bar{u}$). For FCO_2 in forested sites, analysis of variance (ANOVA) shows that the flux magnitude explained 72% of the variance in FCO_2 random error, with an additional 26% accounted for by wind speed. Similarly, at the agricultural and forested sites, both flux magnitude and wind speed account for a significant amount of variation in FCO_2 random error (P<0.001). For LE and H, the flux magnitude explained 50–75% of the variation in flux uncertainty. However, for LE and H, there is no dependence of the random error on wind speed at any of the sites (e.g., for LE, P=0.95, P=0.14, P=0.88 at CBS, DX, and QYZ, respectively; for H, P=0.14, P=0.63, P=0.05, in the same order).

Fig. 2 shows the relationship between flux magnitude and RFEs in FCO_2, LE, and H. The errors are not homogeneous. Further analyses indicate that the RFEs are heteroscedastic and consistently increase with an increasing flux magnitude across all sites. For both CO_2 and energy fluxes at all sites, a linear relationship between the absolute value of flux magnitude and random flux error is observed (Fig. 2, for most sites, R^2>0.9), with an exception for random error in H at the agricultural site. For CO_2, at the forested sites, it appears that the slope of the relationship for $\bar{F}\geq0$ is much higher than that for $\bar{F}\leq0$. Random errors increase by 0.61 μmol m^{-2} s^{-1} for every 1.0 μmol m^{-2} s^{-1} increase in $\bar{F}\geq0$ (CO_2 emission), but by only 0.33 μmol m^{-2} s^{-1} for every 1.0 μmol m^{-2} s^{-1} increase in $\bar{F}\leq0$ (CO_2 uptake). Meanwhile, both the slope and intercept of the linear function vary somewhat according to vegetation type (Table 5). For example, the slope is steeper at the forested sites than at the grassland and agricultural sites, indicating that the random errors increase more rapidly with increases in the flux magnitude at the forested site compared with the grassland and agricultural sites. From what has been illustrated, we can determine that the random error fluxes do not approach 0 as $\bar{F}\rightarrow0$. Therefore, there appears to be an underlying base uncertainty that is present regardless of the size of the flux, one implication of which is that the relative error tends to become small as the flux magnitude becomes larger (Richardson et al., 2006). The non-zero base uncertainty may be related to other factors that influence RFEs in addition to flux magnitude.

After comparing and analyzing the result of RFEs, an exponential relationship can be used to express the relationship between RFEs in FCO_2 and wind speed (Fig. 3). Generally, the higher the wind speed, the smaller the random flux error. Also, the dependence of FCO_2 random error on wind speed varies somewhat according to vegetation type. The relationship between the RFEs of FCO_2 and wind speed can be reasonably well approximated using a function of the form $y = ae^{b(\bar{u})}$, where a=5.71 b=–0.23 (for forested sites, R^2=0.91); a=5.27, b=–0.23 (for grassland sites, R^2=0.86), and a=1.03, b=–0.11 (for agricultural site, R^2=0.65). In forest ecosystems, the ground surface is usually a CO_2 source, and the vegetation community is a CO_2 sink. Therefore, it may need an eddy with low frequency and energy for the complete mixing of the vegetation community and the forest flow system. For a multi-layer system, FCO_2 random flux error strongly depends on wind speed. Dwarf or sparse communities can be considered as a single-layer ecosystem, and thus the random flux error depends less on wind speed. From what has been discussed, we can find that the grassland sites have a relatively flatter exponential curve than that at forested sites. For most of these sites, there is a larger random error at lower wind speed.

3.3. Seasonality of the flux uncertainty

Because of the way in which the random flux error generally correlates with flux magnitude, the random error varies seasonally (Fig. 4). There is a distinct seasonal pattern for the RFEs of FCO_2 and LE, whereas the seasonality of random error in H is not obvious. Generally, the seasonal patterns of RFEs in FCO_2 and LE are similar to the seasonal variation in FCO_2 and LE (Fig. 4). For example, both RFEs and flux magnitude are small in winter months, but they reach the highest value in July and August. The average random error in FCO_2 can reach 3.0 μmol m^{-2} s^{-1} during the growing season (April-September) and less than 1 μmol m^{-2} s^{-1} for the rest of the year. Random error in LE is generally >35 W m^{-2} in the growing season and less than 20 W m^{-2} during other months. By comparison, at all sites, the random error in H is about 25 W m^{-2} throughout the year (with a maximum value in April, i.e., 36.5 W m^{-2}).

Specifically, the random error in FCO_2 and LE at the forested sites is lager than that at the other ecosystem types, except for the maize season in cropland sites (YC). At forested sites, the FCO_2 and LE random error is about three times larger during the growing season than during the rest of the year. At the agricultural site, the seasonal variation of random error in FCO_2 and LE at YC is relatively obvious. There are two peaks in the annual curve (May and August), corresponding to the maize-growing and wheat-growing seasons, respectively, at YC. In three grassland sites, the RFEs remain at low values and with a small peak in the growing season (April–October), which also mimics the seasonal variation in FCO_2 and LE. There is no clear seasonality in the uncertainty of H, indicating that uncertainty for this flux is not modulated by biology; rather, it is totally controlled by physical factors. The uncertainty of LE and FCO_2, however,

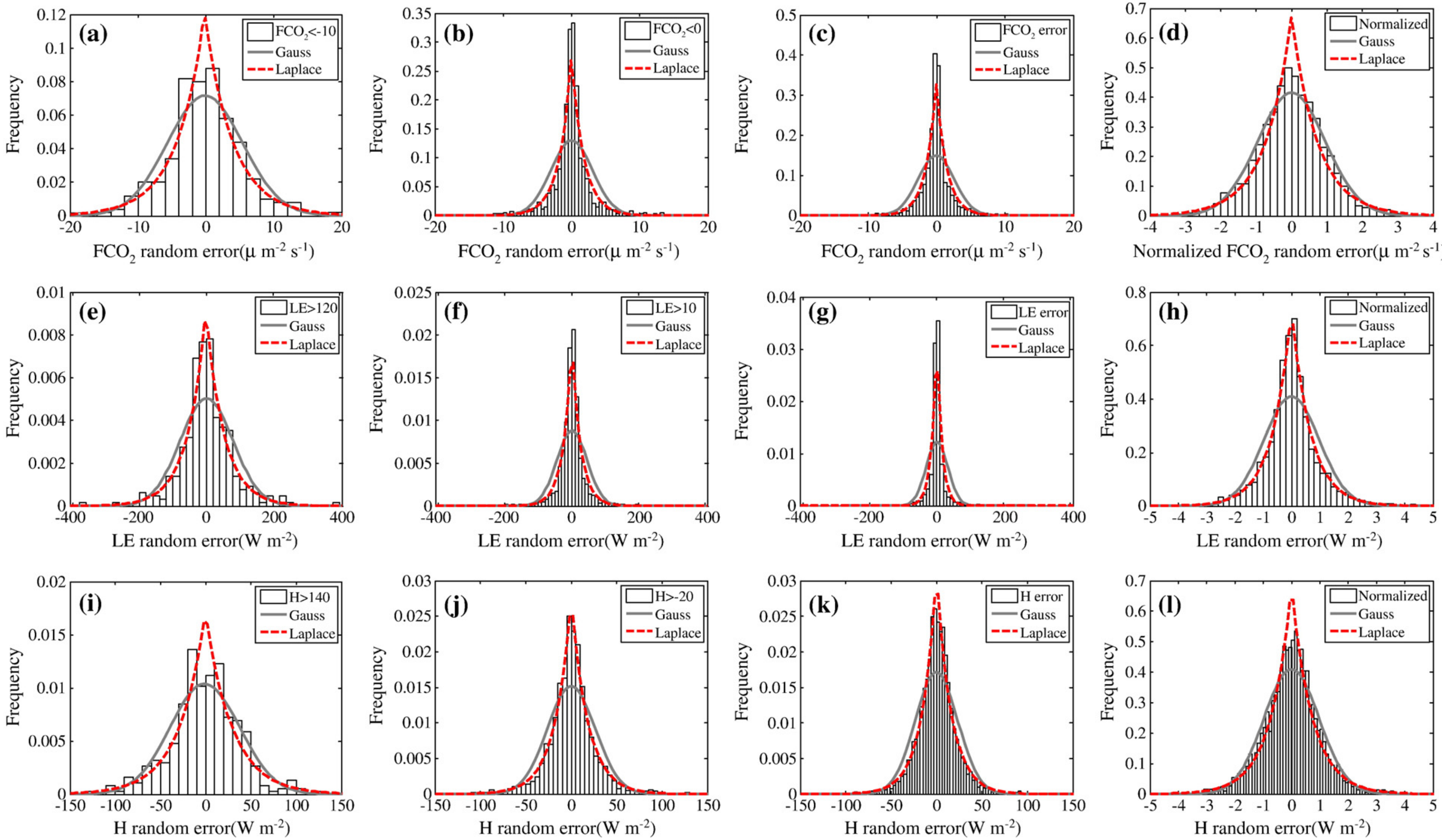

Fig. 1. Distributions of the inferred random flux errors in CO_2 (a–d), LE (e–h), and H (i–l) at CBS site. (a), (e),(i): errors of high flux magnitudes (top 10%); (b), (f), (j): errors of high and medium flux magnitude (top 50%); (c), (g), (k): all inferred errors; (d), (h), (l): errors normalized with standard deviation derived within a time window of seven days.

Table 4
Kurtosis of original (orig) random flux errors and errors normalized (norm) of FCO_2, LE and H.

Site	FCO_2(orig)	FCO_2(norm)	LE(orig)	LE(norm)	H(orig)	H(norm)
CBS	8.53	3.64	12.31	7.03	8.26	4.27
QYZ	15.74	4.43	27.82	5.48	8.97	5.76
HBGC	11.24	3.99	35.08	8.78	22.12	6.78
NM	8.74	3.89	27.22	7.83	32.89	5.68
DX	8.55	3.76	38.34	5.98	183.50	6.19
YC	17.68	4.63	18.01	7.51	9.21	5.04

responds to environment variables differently in the growing and non-growing season, suggesting a biological cause.

As vegetation growth is usually controlled by environment variables such as radiation temperature and precipitation, there appears to be a scaling relationship between radiation (net radiation, R_n and PPFD) and RFEs in FCO_2, LE, and H (Richardson et al., 2006). Here we mainly focus on discussing the influence of temperature on the variance of RFEs, while temperature is the main factor that

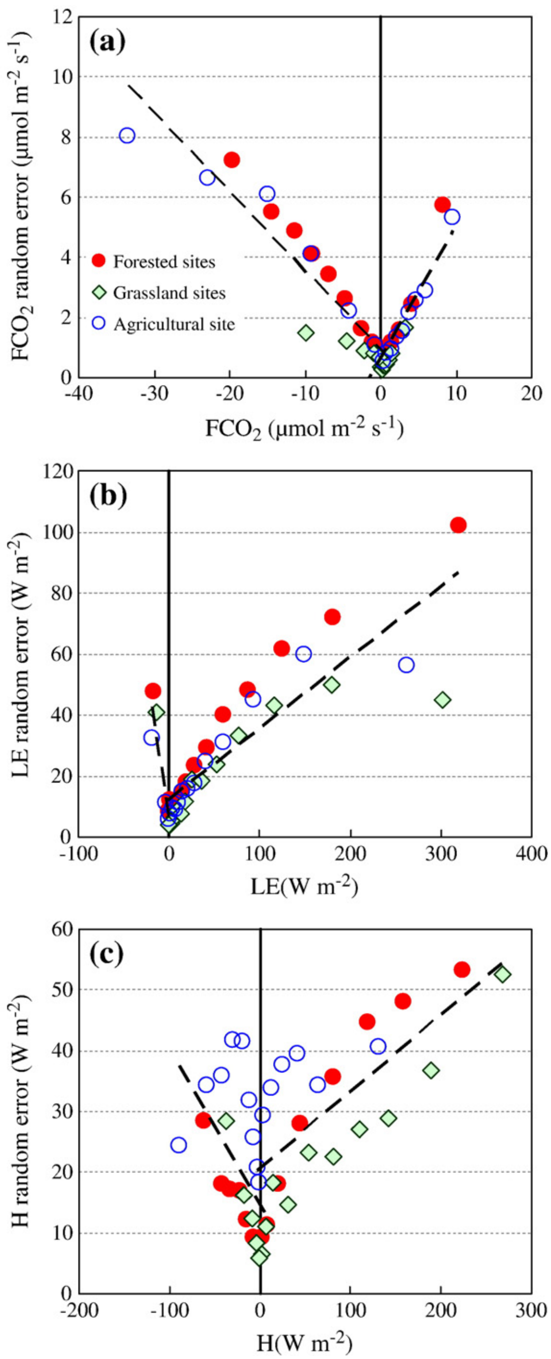

Fig. 2. Scaling of random flux errors of FCO_2(a),LE(b) and H(c)with flux magnitude for three vegetation types. Linear regressions (fit separately for $\overline{F}\geq0$ and $\overline{F}\leq0$) are illustrated.

Table 5
The linear relationship between random flux errors and the flux magnitude.

Flux	Vegetation Type	$\overline{F}\geq0$	$\overline{F}\leq0$
FCO_2	Forested sites	$0.41+0.61FCO_2$ (0.96)	$0.98-0.33FCO_2$ (0.99)
	Grassland Sites	$0.21+0.44FCO_2$ (0.98)	$0.73-0.08FCO_2$ (0.94)
	Agricultural site	$0.29+0.50FCO_2$ (0.98)	$1.70-0.21FCO_2$ (0.92)
LE	Forested sites	$13.86+0.30LE$ (0.96)	$6.00-2.40LE$ (1.00)
	Grassland Sites	$10.79+0.16LE$ (0.75)	$1.86-2.81LE$ (1.00)
	Agricultural site	$11.74+0.22LE$ (0.83)	$7.05-1.41LE$ (1.00)
H	Forested sites	$14.22+0.20H$ (0.91)	$7.63-0.31H$ (0.94)
	Grassland Sites	$10.97+0.15H$ (0.95)	$5.85-0.61H$ (0.99)
	Agricultural site	$33.05+0.06H$ (0.45)	$28.77-0.06H$ (0.04)

Note: Correlation coefficients (R^2) are in brackets.

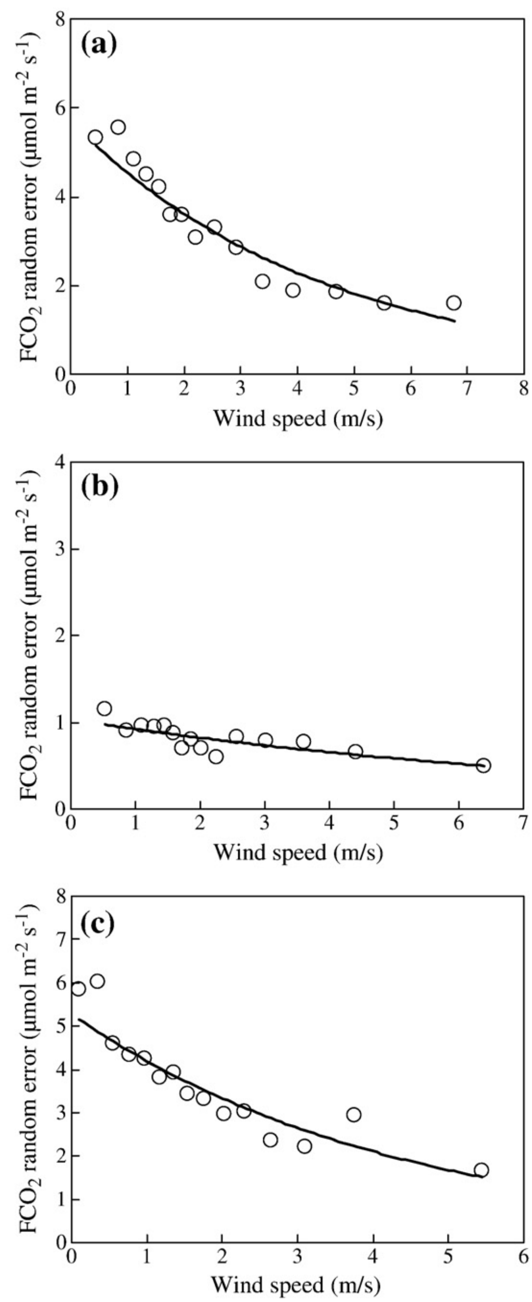

Fig. 3. Scaling of random flux errors in FCO_2 with mean wind speed for three vegetation types. (a) Forested sites; (b) grassland sites; (c) agricultural site.

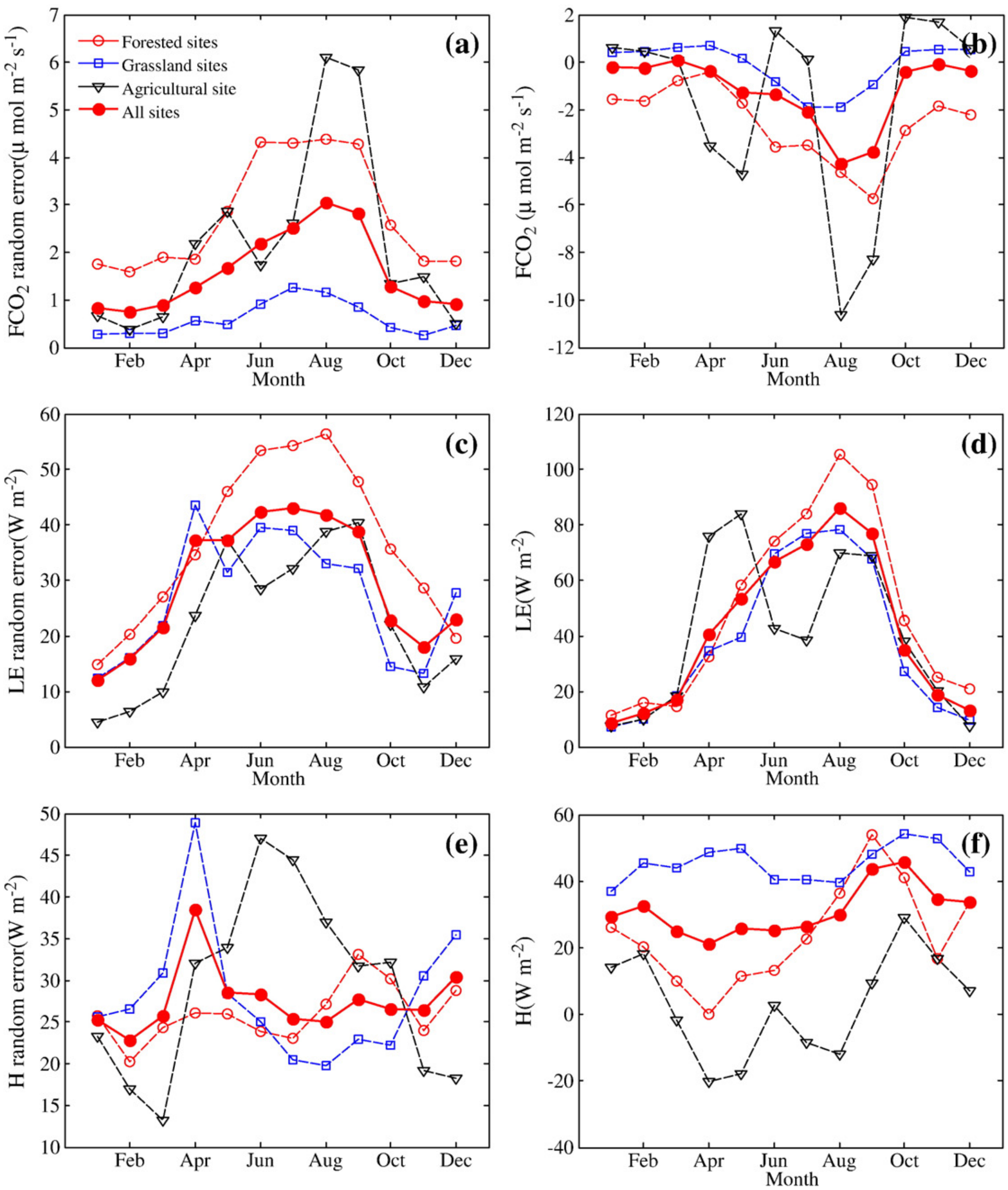

Fig. 4. Seasonality of the random flux errors in FCO_2, LE, and H (a, c, e) and the seasonal variation for FCO_2, LE, and H (b, d, f).

indicates seasonality. The relationship between RFEs for FCO_2, LE, H, and temperature is illustrated in Fig. 5. The results show that the relationship tends to vary somewhat according to vegetation type. In forest ecosystems, for FCO_2, the random error increases as temperature rises within a certain range. When temperature reaches a certain value, RFEs decrease as temperature increases. But this critical value varies with sites (e.g., 21.89 °C at QYZ). In grassland ecosystems, when it comes to alpine meadows in HBGC, there is a consistent correlation between random flux error and temperature, regardless of whether in the growing or dormant season. However, when it comes to NM and DX, there are critical temperatures: 10 °C at DX and 20 °C at NM. In YC farmland ecosystems, due to the phonological reasons, there are completely different tendencies in two seasons: random flux error increases with increasing temperature in the maize-growing season and decreases in the wheat-growing season. For FCO_2, generally, a positive correlation between FCO_2 and temperature can be found, and this relationship may change if there are changes in other environmental variables (e.g., precipitation and radiation). For example, there is often a drought in QYZ and NM during the growing season, and the photosynthesis capacity may be weakened by water deficiency, which in turn leads to a lower net carbon exchange. At DX, an EC tower grassland site located on the Qinghai-Tibet Plateau, similar results can be explained by the dual influences of water deficiency and extra radiation, and the non-monotonic relationship between RFEs in FCO_2 and temperature can be explained by the complex relationship between flux magnitude and temperature. For LE, there tends to be a positive correlation between RFEs and temperature across all sites, as the LE often increases with increasing temperature. For H, the relationship between random flux and temperature is not significant, which coincided with the result in Fig. 4.

Furthermore, as flux magnitude and temperature may be related to each other, partial correlation analysis between RFEs and influencing factor is conducted. At all sites, and for each of FCO_2, LE, and H, the partial correlation coefficient between RFE and temperature is obviously lower than the correlation coefficient ($R>0.6$, $P<0.01$

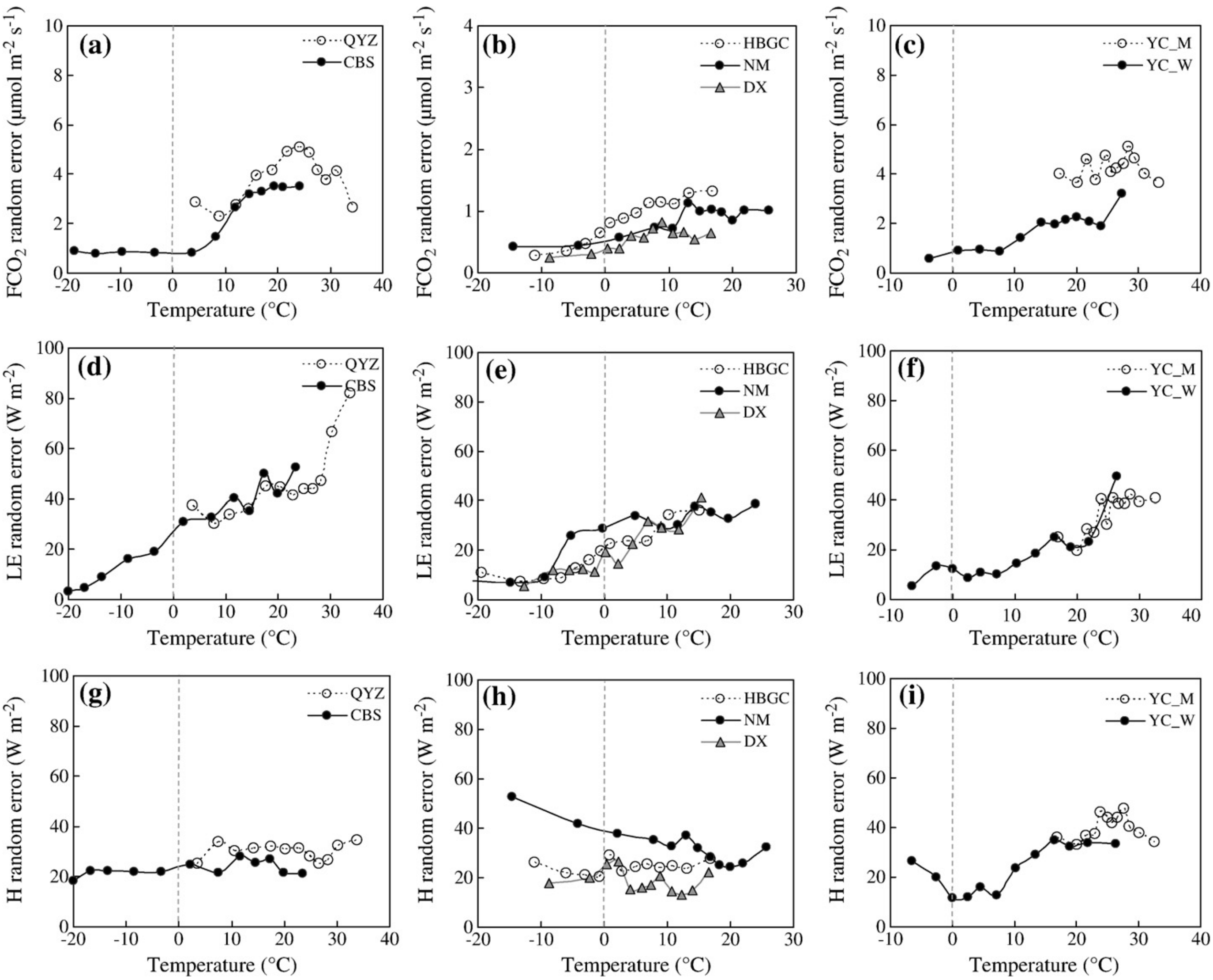

Fig. 5. Relationship between temperature and random flux errors in FCO_2 (left), LE (middle), and H (right) at different vegetation type. (a), (d), (g): forested sites; (b), (e), (h): grassland sites; (c), (f), (i): agricultural site.

at all sites) obtained by a simple linear correlation analysis (Table 6) and even shows no dependence on the random error on temperature at any site (FCO_2: $P=0.42$; $P=0.36$ and $P=0.50$ at YC, QYZ, and NM sites, respectively; LE: $P=0.93$; $P=0.29$, and $P=0.15$ at the same site). Therefore, we conclude that the relationship between environment variables and flux random error is not straightforward. It can be explained by the effect of temperature on flux magnitude, which in turn affects the random flux error.

4. Discussion

4.1. Interpretation of the characteristics of flux uncertainty

The analyses presented here demonstrate that the RFEs in tower-based measurements of CO_2 and energy fluxes are characterized by a non-stationary probability distribution, in that the statistical properties of the errors vary over time and in relation to vegetation type. Generally, the double-exponential distribution provides a better fit with the random error than the normal (Gaussian) distribution, capturing the high peak and thick tail. This is consistent with the results of the repeated-sampling method at two towers in the Howland Forest of AmeriFlux (Hollinger and Richardson, 2005), the repeated-sampling method at single towers at seven sites of AmeriFlux (Hollinger and Richardson, 2005), and the model-residual method in forest ecosystems in CarboEurope (Lasslop et al., 2008; Richardson et al., 2008). In particular, it would appear that while RFEs tend to be approximately Gaussian for high flux measurements (e.g., top 10% of the entire data sets), they are frequently non-Gaussian for low flux measurements. Lasslop et al. (2008) and Stauch et al. (2008) suggest that heteroscedasticity, combined with the varying frequency of different flux magnitude, could result in an error distribution that appears non-Gaussian, and the strongly leptokurtic error distribution is largely due to a superposition of Gaussian distribution for high flux magnitude. These distributions may have resulted from several factors. First, for all fluxes, the data are not constant, and when this heteroscedasticity is combined with the frequency of different flux magnitudes (the instances of low values are far more frequent than of high values), a strongly peaked error distribution may result. The second factor leading to the non-normal error distribution is related to the measurement system (Press et al., 1993). Although the observational errors for most natural phenomena follow a normal distribution, the possibility of other distribution cannot be ruled out. The measurement system is carefully maintained by researchers, however occasionally "glitches" caused by power fluctuations can

Table 6
Correlation matrix for random flux errors in FCO_2, LE, and H, flux magnitude, and temperature.

Site		FCO_2			LE			H		
		$\sigma(\delta)$	|F|	T	$\sigma(\delta)$	|F|	T	$\sigma(\delta)$	|F|	T
QYZ	$\sigma(\delta)$	1.00	$\underline{0.95}^{**}$	$\underline{0.26}$	1.00	$\underline{0.80}^{**}$	$\underline{0.62}^{**}$	1.00	$\underline{0.94}^{**}$	$\underline{-0.58}^{**}$
	|F|	0.99^{**}	1.00	0.93^{**}	0.98^{**}	1.00	0.94^{**}	0.95^{**}	1.00	0.83^{**}
	T	0.93^{**}	0.93^{**}	1.00	0.96^{**}	0.94^{**}	1.00	0.68	0.83^{**}	1.00
CBS	$\sigma(\delta)$	1.00	$\underline{0.99}^{**}$	$\underline{-0.56}^{**}$	1.00	$\underline{0.88}^{**}$	$\underline{-0.30}$	1.00	$\underline{0.92}^{**}$	$\underline{0.17}$
	|F|	1.00^{**}	1.00	0.87^{**}	0.95^{**}	1.00	0.87^{**}	0.93^{**}	1.00	0.42
	T	0.84^{**}	0.87^{**}	1.00	0.78^{**}	0.87^{**}	1.00	0.45	0.42	1.00
HBGC	$\sigma(\delta)$	1.00	$\underline{-0.39}$	$\underline{0.77}^{**}$	1.00	$\underline{-0.15}$	$\underline{0.57}^{**}$	1.00	$\underline{0.37}$	$\underline{0.78}^{**}$
	|F|	0.86^{**}	1.00	0.96^{**}	0.85^{**}	1.00	0.96^{**}	0.48	1.00	0.34
	T	0.94^{**}	0.96^{**}	1.00	0.90^{**}	0.96^{**}	1.00	0.81^{**}	0.34	1.00
DX	$\sigma(\delta)$	1.00	$\underline{0.55}^{**}$	$\underline{0.20}$	1.00	$\underline{0.88}^{**}$	$\underline{-0.53}$	1.00	$\underline{0.78}^{**}$	$\underline{0.89}^{**}$
	|F|	0.92^{**}	1.00	0.93^{**}	0.96^{**}	1.00	0.94^{**}	0.87^{**}	1.00	0.73^{**}
	T	0.88^{**}	0.93^{**}	1.00	0.85^{**}	0.94^{**}	1.00	0.94^{**}	0.73^{**}	1.00
NM	$\sigma(\delta)$	1.00	$\underline{0.93}^{**}$	$\underline{-0.20}$	1.00	$\underline{0.88}^{**}$	$\underline{-0.41}$	1.00	$\underline{0.94}^{**}$	$\underline{0.85}^{**}$
	|F|	0.98^{**}	1.00	0.87^{**}	0.97^{**}	1.00	0.94^{**}	0.95^{**}	1.00	0.71^{**}
	T	0.83^{**}	0.87^{**}	1.00	0.87^{**}	0.94^{**}	1.00	0.86^{**}	0.71^{**}	1.00
YC	$\sigma(\delta)$	1.00	$\underline{0.93}^{**}$	$\underline{-0.24}$	1.00	$\underline{0.65}^{**}$	$\underline{-0.03}$	1.00	$\underline{-0.25}$	$\underline{0.79}^{**}$
	|F|	0.96^{**}	1.00	0.74^{**}	0.90^{**}	1.00	0.92^{**}	0.41	1.00	0.64^{**}
	T	0.67^{**}	0.74^{**}	1.00	0.82^{**}	0.92^{**}	1.00	0.82^{**}	0.64^{**}	1.00

Pair-wise correlation coefficients are shown in the lower triangle, while partial correlation coefficients are shown with underline; $\sigma(\delta)$: Random flux error, |F|: flux magnitude, T : temperature. The level of significance is indicated ($^{**}P<0.05$).

occur, and contamination of other factors results in measurements that are far from accurate, which collectively leads to a non-normal distribution (Hollinger and Richardson, 2005).

From this study, we find that the manner in which the random errors of three fluxes in ChinaFLUX scales with the flux magnitude is similar to that presented previously (e.g., Hollinger and Richardson, 2005; Richardson et al., 2006; Stauch et al., 2008). The linear relationship between RFEs and flux magnitude is consistent in ChinaFLUX, AmeriFlux, and CarboEurope (Table 4). Meanwhile, the linear relationship varies somewhat according to ecosystem type, and RFEs in forested sites are more influenced by flux magnitude than grassland ecosystems. Whereas the relationship between RFEs in FCO_2 and flux magnitude is similar with the same vegetation type, with little difference in the slope and intercept. Richardson et al. (2008) point out that the non-zero intercept in Fig. 2 and Table 5 means that large-magnitude fluxes have a better signal-to-noise ratio and will still exert a greater influence during the optimization than small fluxes.

We also find that, with the single-tower repeated-sampling method in ChinaFLUX and AmeriFlux, the variance degree of random error in FCO_2 and flux magnitude for $\overline{F}\geq 0$ (CO_2 emission) is higher than that for $\overline{F}\leq 0$ (CO_2 uptake) (Table 7). However, this phenomenon does not occur in forest ecosystem of CarboEurope, regardless of the use of the daily-differencing method or model-residual method. The most probable reason is the pre-processing of flux data (e.g., the determination of u^* and the standard for rejecting abnormal value, etc.), as there is a stricter pre-processing standard in CarboEurope than that in ChinaFLUX and AmeriFlux (Richardson et al., 2008). In conclusion, flux magnitude could be one of the main reasons driving flux uncertainty, which may be influenced mainly by the intermittent turbulence transmission, rather than the measurement system (ultrasonic apparatus and gas analyzer etc.). This tendency is similar to the result of the error model by Mann and Lenschow (1994).

The dependence of FCO_2 random error on wind speed varies somewhat according to vegetation type. FCO_2 random error decreases dramatically at high wind speeds for most sites, which is consistent with the theory of Mann and Lenschow (1994). The phenomenon may be explained by the fact that high wind speeds lead to sufficient turbulent transport between ecosystem and the atmosphere, and measurements taken during greater turbulence are closer to the actual value than those obtained at low wind speeds. Because of the way in which the random flux error generally correlates with flux magnitude, the random error varies seasonally. As temperature is the main limiting factor of vegetation growth, there tends to be a relationship between RFEs and temperature. However, partial correlation analysis shows that there is no significant relationship between RFEs and temperature, which further demonstrates that the flux magnitude is a primary factor influencing the variance of RFEs.

4.2. Influence of CO_2 flux uncertainty on model parameter estimate and CO_2 components

Studies have shown that observation uncertainty has significant impact on model parameter estimates and predictions (Richardson and Hollinger, 2005; Trudinger et al., 2007; Lasslop et al., 2008; Zhang et al., 2008; Liu et al., 2009).According to the results of ChinaFLUX and previous studies in AmeriFlux, and CarboEurope (Richardson et al.,

Table 7
Comparison of the relationship between CO_2 flux random error and flux magnitude among ChinaFLUX, AmeriFlux, CarbonEurope for different ecosystems.

Flux	Ecosystem type	ChinaFLUX (daily-differencing approach) (this study)		AmeriFlux (daily-differencing approach) (Richardson et al., 2006)		CarbonEurope (Richardson et al., 2008)	
		$\overline{F}\geq 0$	$\overline{F}\leq 0$	$\overline{F}\geq 0$	$\overline{F}\leq 0$	Daily-differencing approach	Model residual approach
FCO_2	Forest	$0.41+0.61FCO_2$	$0.98-0.33FCO_2$	$0.62+0.63FCO_2$	$1.42-0.19FCO_2$	$1.47+0.12\|FCO_2\|$	$1.69+0.16\|FCO_2\|$
	Grassland	$0.21+0.44FCO_2$	$0.73-0.08FCO_2$	$0.38+0.30\ FCO_2$	$0.47-0.2FCO_2$	–	–
	Agriculture	$0.29+0.50FCO_2$	$1.70-0.21FCO_2$	–	–	–	–
LE	Forest	$13.86+0.30LE$	$6.00-2.40LE$	$15.3+0.23LE$	$6.2-1.42LE$	–	–
	Grassland	$10.79+0.16LE$	$1.86-2.81LE$	$8.1+0.16LE$	No data	–	–
	Agriculture	$11.74+0.22LE$	$7.05-1.41LE$	–	–	–	–
H	Forest	$14.22+0.20H$	$7.63-0.31H$	$19.7+0.16H$	$10-0.44\ H$	–	–
	Grassland	$10.97+0.15H$	$5.85-0.61H$	$17.3+0.07H$	$13.3-0.16H$	–	–
	Agriculture	$33.05+0.06H$	$28.77-0.06H$	–	–	–	–

2006, 2008; Lasslop et al., 2008), RFEs are characterized by non-stationary probability distributions, in that the statistical properties of the error vary over time and in relation to the magnitude of the flux. The non-normality and homoscedasticity in RFEs provide a solid foundation for implementing a weighted optimization scheme in conducting model-data syntheses, whereby observations measured with greater confidence (lower standard deviation) receive more weight during the optimization (i.e., in the cost function) than observations measured with less confidence.

Ordinary least-square fitting can yield maximum likelihood parameter estimates when the data meet the assumption of normality and homoscedasticity. However, when these assumptions are not met, other data-fitting methods should be used. Given the double-exponential distribution of RFEs, maximum-likelihood fitting should be based on minimizing the sum of the absolute deviation. A key difference between the least-square criterion and the absolute deviation criterion is that, with least squares, outliers exert a much stronger influence on the fit, because the deviations are minimized. Thus, outliers, which may have no biological significance, should not be given undue weight. Lasslop et al. (2008) also suggest that the proper implementation of the random error standard deviation scaling with flux magnitude can significantly reduce the parameter uncertainty and often yield parameter retrievals that are closer to the true value than by using ordinary least squares. In addition, the physiological parameters derived from eddy covariance data are very useful for scaling exercises and model-data synthesis (Xiao et al., 2004; Wang et al., 2007; Williams et al., 2009). Therefore, knowledge of the random errors in half-hourly flux measurement is critical for parameter estimation and gap-filling of flux data. Meanwhile, flux uncertainty information is also necessary for evaluating the accumulated flux and uncertainty in temporal integrated (daily, monthly, and annual) fluxes.

Knowledge of flux uncertainty is important for evaluating independently formulated models against flux data and also necessary for model-data synthesis (i.e., data assimilation). How to adopt an effective method to reduce the uncertainty of measurements and to improve the prediction of flux exchange between ecosystem and the atmosphere is essential for global-change studies. Therefore, future work is needed to further integrate sources of uncertainty, evaluate alternate modeling techniques, and generalize results across multiple sites.

5. Conclusions

In this study, we use the daily-differencing approach to conduct an uncertainty analysis of CO_2 and energy flux measurements. Results from six eddy covariance tower sites in ChinaFLUX have been used to show that the distribution of RFEs in FCO_2, LE, and H appears to follow a double-exponential distribution, rather than normal distribution, which is basically in accord with the results in AmeriFlux and CarboEurope. Meanwhile, this strongly leptokurtic error distribution is revealed to be largely due to a superposition of Gaussian distribution for high flux magnitude. Furthermore, the standard deviation of RFEs is not constant, but heteroscedastic with the magnitude of the flux, and it varies as a function of environment variables (e.g., wind speed for FCO_2). Because the random error is non-normal and heteroscedastic (non-constant), the two assumptions (i.e., normality and homoscedasticity) of ordinary least-squares optimization is no longer met, and the ordinary least squares need to be extended to weighted least squares or other data-fitting methods based on minimizing the sum of the absolute deviation. We also show that the RFEs vary from site to site and are somewhat related to vegetation type. There is an obvious seasonality pattern of RFEs in FCO_2 and LE, but not in H, and the variation of RFEs can be primarily attributed to the flux magnitude. Environment variables (e.g., temperature) affect RFEs by changing the flux magnitude.

Acknowledgements

This research was supported the National Key Basic Research and Development Program (Grant No. 2010CB833504), by the Information Project and the Directionality Project, Chinese Academy of Sciences (Grant No. KZCX2-YW-433-06), and the Monumental Projects (Grant Nos.30590381 and 30570347) of the National Science Foundation of China. We would like to thank the anonymous reviewers for their comments, which have greatly helped to improve the manuscript.

References

Baldocchi, D., Falge, E., Gu, L.H., Olson, R., Hollinger, D., Running, S., Anthoni, P., Bernhofer, C., Davis, K., Evans, R., Fuentes, J., Goldstein, A., Katul, G., Law, B., Lee, X.H., Malhi, Y., Meyers, T., Munger, W., Oechel, W., U, K. T. P., Pilegaard, K., Schmid, H.P., Valentini, R., Verma, S., Vesala, T., Wilson, K., Wofsy, S., 2001. FLUXNET: A new tool to study the temporal and spatial variability of ecosystem-scale carbon dioxide, water vapor, and energy flux densities. Bulletin of the American Meteorological Society 82, 2415–2434.

Baldocchi, D.D., 2003. Assessing the eddy covariance technique for evaluating carbon dioxide exchange rates of ecosystems: past, present and future. Global Change Biology 9, 479–492.

Chevallier, F., Viovy, N., Reichstein, M., Ciais, P., 2006. On the assignment of prior errors in Bayesian inversions of CO_2 surface fluxes. Geophysical Research Letters 33. doi:10.1029/2006gl026496.

Friend, A.D., Arneth, A., Kiang, N.Y., Lomas, M., Ogee, J., Rodenbeckk, C., Running, S.W., Santaren, J.D., Sitch, S., Viovy, N., Woodward, F.I., Zaehle, S., 2007. FLUXNET and modelling the global carbon cycle. Global Change Biology 13, 610–633.

Goulden, M.L., Munger, J.W., Fan, S.M., Daube, B.C., Wofsy, S.C., 1996. Measurements of carbon sequestration by long-term eddy covariance: methods and a critical evaluation of accuracy. Global Change Biology 2, 169–182.

Hagen, S.C., Braswell, B.H., Linder, E., Frolking, S., Richardson, A.D., Hollinger, D.Y., 2006. Statistical uncertainty of eddy flux-based estimates of gross ecosystem carbon exchange at Howland Forest, Maine. Journal of Geophysical Research-Atmospheres 111 (D08S03). doi:10.1029/2005JD006154.

Hollinger, D.Y., Kelliher, F.M., Byers, J.N., Hunt, J.E., Mcseveny, T.M., Weir, P.L., 1994. Carbon-dioxide exchange between an undisturbed old-growth temperate forest and the atmosphere. Ecology 75, 134–150.

Hollinger, D.Y., Richardson, A.D., 2005. Uncertainty in eddy covariance measurements and its application to physiological models. Tree Physiol 25, 873–885.

Lasslop, G., Reichstein, M., Kattge, J., Papale, D., 2008. Influences of observation errors in eddy flux data on inverse model parameter estimation. Biogeosciences 5, 1311–1324.

Lenschow, D.H., Mann, J., Kristensen, L., 1994. How long is long enough when measuring fluxes and other turbulence statistics. Journal of Atmospheric and Oceanic Technology 11, 661–673.

Leuning, R., 2004. Measurements of trace gas fluxes in the atmosphere using eddy covariance: WPL corrections revisited. In: Lee, X., Massman, W., Law, B. (Eds.), Handbook of Micrometeorology:A Guide for Surface Flux Measurement and Analysis. Kluwer Academic Publisher, Dordrecht, pp. 119–132.

Li, C., He, H.L., Liu, M., et al., 2008. The design and application of CO2 flux data processing system at ChinaFLUX. Geo-Information Science 10 (5), 557–565 (in Chinese with English abstract).

Liu, M., He, H.L., Yu, G.R., Luo, Y.Q., Sun, X.M., Wang, H.M., 2009. Uncertainty analysis of CO2 flux components in subtropical evergreen coniferous plantation. Science in China Series D-Earth Sciences 52, 257–268.

Mahrt, L., 1998. Flux sampling errors for aircraft and towers. Journal of Atmospheric and Oceanic Technology 15, 416–429.

Mann, J., Lenschow, D.H., 1994. Errors in airborne flux measurements. Journal of Geophysical Research-Atmospheres 99, 14519–14526.

Massman, W.J., Lee, X., 2002. Eddy covariance flux corrections and uncertainties in long-term studies of carbon and energy exchanges. Agricultural and Forest Meteorology 113, 121–144.

Mizoguchi, Y., Miyata, A., Ohtani, Y., Hirata, R., Yuta, S., 2009. A review of tower flux observation sites in Asia. Journal of Forest Research 14, 1–9.

Moncrieff, J.B., Malhi, Y., Leuning, R., 1996. The propagation of errors in long-term measurements of land-atmosphere fluxes of carbon and water. Global Change Biology 2, 231–240.

Morgenstern, K., Black, T.A., Humphreys, E.R., Griffis, T.J., Drewitt, G.B., Cai, T.B., Nesic, Z., Spittlehouse, D.L., Livingstone, N.J., 2004. Sensitivity and uncertainty of the carbon balance of a Pacific Northwest Douglas-fir forest during an El Nino La Nina cycle. Agricultural and Forest Meteorology 123, 201–219.

Papale, D., Reichstein, M., Aubinet, M., Canfora, E., Bernhofer, C., Kutsch, W., Longdoz, B., Rambal, S., Valentini, R., Vesala, T., Yakir, D., 2006. Towards a standardized processing of Net Ecosystem Exchange measured with eddy covariance technique: algorithms and uncertainty estimation. Biogeosciences 3, 571–583.

Press, W.H., Flannery, B.P., Teukolsky, S.A., Vetterling, W.T., 1993. Numerical recipes in Fortran 77: the art of scientific computing. Cambridge University Press, New York. 992 pp.

Rannik, U., Kolari, P., Vesala, T., Hari, P., 2006. Uncertainties in measurement and modelling of net ecosystem exchange of a forest. Agricultural and Forest Meteorology 138, 244–257.

Raupach, M.R., Rayner, P.J., Barrett, D.J., DeFries, R.S., Heimann, M., Ojima, D.S., Quegan, S., Schmullius, C.C., 2005. Model-data synthesis in terrestrial carbon observation: methods, data requirements and data uncertainty specifications. Global Change Biology 11, 378–397.
Reichstein, M., Falge, E., Baldocchi, D., Papale, D., Aubinet, M., Berbigier, P., Bernhofer, C., Buchmann, N., Gilmanov, T., Granier, A., Grunwald, T., Havrankova, K., Ilvesniemi, H., Janous, D., Knohl, A., Laurila, T., Lohila, A., Loustau, D., Matteucci, G., Meyers, T., Miglietta, F., Ourcival, J.M., Pumpanen, J., Rambal, S., Rotenberg, E., Sanz, M., Tenhunen, J., Seufert, G., Vaccari, F., Vesala, T., Yakir, D., Valentini, R., 2005. On the separation of net ecosystem exchange into assimilation and ecosystem respiration: review and improved algorithm. Global Change Biology 11, 1424–1439.
Richardson, A.D., Hollinger, D.Y., 2005. Statistical modeling of ecosystem respiration using eddy covariance data: maximum likelihood parameter estimation, and Monte Carlo simulation of model and parameter uncertainty, applied to three simple models. Agricultural and Forest Meteorology 131, 191–208.
Richardson, A.D., Hollinger, D.Y., Burba, G.G., Davis, K.J., Flanagan, L.B., Katul, G.G., Munger, J.W., Ricciuto, D.M., Stoy, P.C., Suyker, A.E., Verma, S.B., Wofsy, S.C., 2006. A multi-site analysis of random error in tower-based measurements of carbon and energy fluxes. Agricultural and Forest Meteorology 136, 1–18.
Richardson, A.D., Mahecha, M.D., Falge, E., Kattge, J., Moffat, A.M., Papale, D., Reichstein, M., Stauch, V.J., Braswell, B.H., Churkina, G., Kruijt, B., Hollinger, D.Y., 2008. Statistical properties of random CO2 flux measurement uncertainty inferred from model residuals. Agricultural and Forest Meteorology 148, 38–50.
Stauch, V.J., Jarvis, A.J., Schulz, K., 2008. Estimation of net carbon exchange using eddy covariance CO2 flux observations and a stochastic model. Journal of Geophysical Research-Atmospheres 113 (D3), D03101. doi:10.1029/2007jd008603.
Trudinger, C.M., Raupach, M.R., Rayner, P.J., Kattge, J., Liu, Q., Pak, B., Reichstein, M., Renzullo, L., Richardson, A.D., Roxburgh, S.H., Styles, J., Wang, Y.P., Briggs, P., Barrett, D., Nikolova, S., 2007. OptIC project: an intercomparison of optimization techniques for parameter estimation in terrestrial biogeochemical models. Journal of Geophysical Research-Biogeosciences 112 (G2), G02027. doi:10.1029/2006jg000367.
Twine, T.E., Kustas, W.P., Norman, J.M., Cook, D.R., Houser, P.R., Meyers, T.P., Prueger, J.H., Starks, P.J., Wesely, M.L., 2000. Correcting eddy-covariance flux underestimates over a grassland. Agricultural and Forest Meteorology 103, 279–300.
Wang, Y.P., Baldocchi, D., Leuning, R., Falge, E., Vesala, T., 2007. Estimating parameters in a land-surface model by applying nonlinear inversion to eddy covariance flux measurements from eight FLUXNET sites. Global Change Biology 13, 652–670.
Webb, E.K., Pearman, G.I., Leuning, R., 1980. Correction of flux measurements for density effects due to heat and water-vapor transfer. Quarterly Journal of the Royal Meteorological Society 106, 85–100.
Wilczak, J.M., Oncley, S.P., Stage, S.A., 2001. Sonic anemometer tilt correction algorithms. Boundary-Layer Meteorology 99, 127–150.
Williams, M., Richardson, A.D., Reichstein, M., Stoy, P.C., Peylin, P., Verbeeck, H., Carvalhais, N., Jung, M., Hollinger, D.Y., Kattge, J., Leuning, R., Luo, Y., Tomelleri, E., Trudinger, C.M., Wang, Y.-P., 2009. Improving land surface models with FLUXNET data. Biogeosciences 7, 1341–1359.
Xiao, X.M., Hollinger, D., Aber, J., Goltz, M., Davidson, E.A., Zhang, Q.Y., Moore, B., 2004. Satellite-based modeling of gross primary production in an evergreen needleleaf forest. Remote Sensing of Environment 89, 519–534.
Yu, G.R., Wen, X.F., Sun, X.M., Tanner, B.D., Lee, X.H., Chen, J.Y., 2006. Overview of ChinaFLUX and evaluation of its eddy covariance measurement. Agricultural and Forest Meteorology 137, 125–137.
Zhang, L., Yu, G., Luo, Y., Gu, F., Zhang, L., 2008. Influences of error distributions of net ecosystem exchange on parameter estimation of a process-based terrestrial model: a case of broad-leaved Korean pine mixed forest in Changbaishan, China. Acta Ecologica Sinica 28, 3017–3026.